Available online at www.sciencedirect.com
SCIENCE DIRECT
Catalysis Today 111 (2006) 52–58
CATALYSIS TODAY
www.elsevier.com/locate/cattod

Near-surface alloys for hydrogen fuel cell applications

Jeff Greeley [a,b], Manos Mavrikakis [a,*]

[a] Department of Chemical and Biological Engineering, University of Wisconsin-Madison, Madison, WI 53706, USA
[b] Center for Atomic-Scale Materials Physics, Department of Physics, Technical University of Denmark, DK-2800 Kongens Lyngby, Denmark

Available online 18 November 2005

Abstract

Near-surface alloys (NSAs) possess a variety of unusual catalytic properties that could make them useful candidates for improved catalysts in a variety of chemical processes. It is known from previous work, for example, that some NSAs bind hydrogen very weakly while, at the same time, permitting facile H_2 activation. These NSAs could, potentially, facilitate highly selective hydrogenation reactions at low temperatures. In the present work, the suitability of NSAs for use as hydrogen fuel cell anodes has been evaluated; the combination of properties, possessed by selected NSAs, of weak binding of CO with relatively facile H_2 activation is nearly ideal for this application. We suggest that, as nanoscale materials synthesis techniques improve, it will become feasible to reproducibly prepare NSAs with highly specified surface structures, resulting in the design and manufacture of a wide variety of such materials for use in fuel cells and in an ever-increasing range of catalytic applications. Furthermore, we introduce a new concept for NSA-defect sites, which could be responsible for the promotional catalytic effects of a second metal added, even in minute quantities, to a host metal catalyst.

Keywords: Density functional theory; Hydrogen; Carbon monoxide; Fuel cells; Anodes; Metals; Alloys; Atomic layer deposition; Defect sites

1. Introduction

The rational design of catalysts has been a long-standing goal of surface scientists and engineers [1,2], and recent investigations have begun to uncover some of the principles necessary for these types of design efforts to be successful [3–5]. Certain of these investigations concern the role that near-surface alloys (NSAs) can play in endowing surfaces with novel catalytic properties. NSAs are alloys where a solute metal is present near the surface of a host metal in concentrations different from the bulk. Although NSAs may contain only a minute amount of solute in the surface region of the catalysts, they can have catalytic properties that differ dramatically from the properties of the corresponding pure metals [6–9].

Although studies of *individual* NSAs are becoming increasingly common [10–12], there has still been relatively little work done to elucidate trends in the properties of NSAs for a broad *range* of transition metals and adsorbates. First-principles computational methods [13] offer an ideal framework for the development of such trends, as those methods permit the screening of a large number of different NSAs at relatively low cost. Computational studies of the thermochemical [14,15] and kinetic [16] properties of hydrogen on a variety of different NSA surfaces have confirmed the generality of the surprising catalytic properties discussed in the individual cases above. Studies of H_2 dissociation kinetics, in particular, have shown very surprising results; they demonstrated that some NSAs can produce a combination of weak atomic hydrogen (H) binding and facile H_2 dissociation [16]. For H_2 dissociation, weak binding of H would typically be thought to imply a *high* H_2 activation energy barrier [17–20]. However, certain NSAs were shown to offer exceptions to this rule by simultaneously allowing weak H binding and *low* H_2 dissociation barriers. Weak binding of H, in turn, could facilitate subsequent hydrogen-transfer reaction steps, allowing lower temperatures to be employed for reactions on these NSAs, and thereby, enhancing the selectivity of related processes.

The success of computational studies in revealing unique NSA properties for hydrogen-related applications suggests that a similar study of adsorbates and properties that are of interest for the design of hydrogen fuel cell anodes might prove fruitful. It has long been known that pure hydrogen is an ideal fuel cell feed; on platinum anodes, for example, nearly no voltage loss is

* Corresponding author. Tel.: +1 608 262 9053; fax: +1 608 262 5434.
E-mail address: manos@engr.wisc.edu (M. Mavrikakis).

0920-5861/$ – see front matter
doi:10.1016/j.cattod.2005.10.009

observed when hydrogen is employed [21]. However, due to the steam reforming process used to produce hydrogen, small amounts of carbon monoxide are always present in hydrogen feed streams [22]. In turn, even trace amounts of CO effectively poison the platinum anode surface, leading to deactivation of the fuel cell.

Given the above considerations, it would be highly desirable to find alloys for anodes that would be resistant to CO poisoning. CO-resistant materials could be created, for example, simply by finding alloys that bind CO very weakly. This approach must be used with care because, as will be shown here, alloys that bind CO weakly often bind atomic hydrogen weakly, as well, and weak binding of atomic hydrogen often implies difficulty in activating the H_2 bond. NSAs, however, might be ideally suited to overcome these limitations. In particular, the ability of some NSAs to activate H_2 while, at the same time, binding atomic hydrogen and CO weakly could make them ideal candidates for hydrogen fuel cell anodes. Additionally, the low temperatures used in fuel cells would facilitate the stabilization of metastable NSAs, thus broadening the range of NSAs that might be useful for fuel cell applications.

In this contribution, we begin by summarizing previous results concerning hydrogen adsorption on NSAs. We then present a database of binding energies of CO on various NSAs, and we demonstrate the existence of a correlation between the CO and hydrogen binding energies. Subsequently, we show how these data can be combined with information about the kinetics of H_2 bond scission on NSAs to identify promising candidates for hydrogen fuel cell anodes. Finally, we introduce and discuss the unusual properties of a new kind of highly active catalytic defect site, which we call NSA-defect site.

2. Methods

DACAPO, the total energy calculation code [23], is used in this study. For all calculations, a four-layer slab, periodically repeated in a super-cell geometry with five equivalent layers of vacuum between any two successive metal slabs, is used. A 2×2 unit cell is employed, and the top two layers of the slab are allowed to relax. Adsorption is allowed on only one of the two surfaces exposed, and the electrostatic potential is adjusted accordingly [24]. Ionic cores are described by ultrasoft pseudopotentials [25], and the Kohn-Sham one-electron valence states are expanded in a basis of plane waves with kinetic energy below 25 Ry. The surface Brillouin zone of close-packed metal surfaces is sampled at 18 special Chadi-Cohen k points; bcc(1 1 0) surfaces are sampled with a $4 \times 4 \times 1$ Monkhorst-Pack k-point grid. In all cases, convergence of the total energy with respect to the k point set and with respect to the number of metal layers included is confirmed. The exchange-correlation energy and potential are described self-consistently within the generalized gradient approximation (GGA-PW91) [26,27]. The self-consistent PW91 density is determined by iterative diagonalization of the Kohn-Sham Hamiltonian, Fermi population of the Kohn-Sham states ($k_BT = 0.1$ eV), and Pulay mixing of the resulting electronic density [28]. All total energies have been extrapolated to

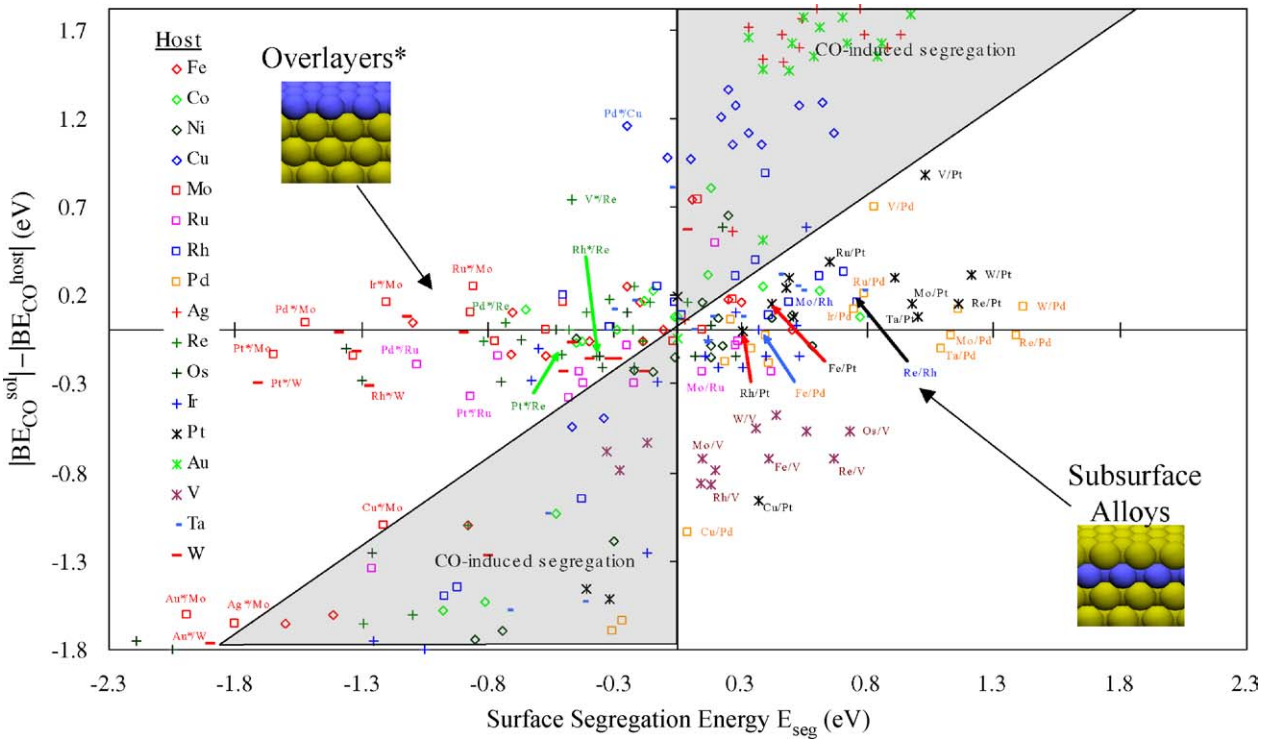

Fig. 1. Stability of NSAs with respect to carbon monoxide-induced segregation. Metal alloys are denoted as *solute/host* pairs. The x-axis indicates the energy (“surface segregation”) for a single solute atom to move from the bulk to the surface layer of the host metal. The y-axis denotes the difference between the magnitudes of the CO binding energies (θ_{CO} = 1/4ML) on the pure solute and on the pure host close-packed metal surfaces. Regions in which CO-induced segregation is expected are shaded. The insets show the structure of overlayer and subsurface alloy NSAs.

$k_BT = 0$ eV. Zero-point energy effects are not considered in the reported results. Spin polarization effects are tested for and included where appropriate.

The structures of the idealized NSAs considered in this study are described with the notation "X*/Y" or "X/Y". In both cases, X refers to the solute metal, and Y denotes the host metal. A superscript asterisk (*) indicates that the solute is present in the form of an overlayer; the absence of an asterisk indicates that the solute forms a subsurface alloy (see insets of Fig. 1). In both cases, the total coverage of the solute is one monolayer.

The calculated PW91 bond energy for H_2(g) is 4.57 eV. This result implies a zero-point energy corrected value of ~4.30 eV, in fair agreement with the experimental value of 4.52 eV at 298 K [29].

3. Results

In this section, we first comment briefly on the stability of NSAs in hydrogen- and CO-rich environments. We then review previously published results for H_2 dissociation and H adsorption on various pure metals and NSAs, focusing on the unusual properties of NSAs that may provide improved activity and stability for catalytic processes involving hydrogen. Next, we present new results for CO adsorption on a variety of NSAs. Finally, we combine the hydrogen and CO results in an attempt to assess the suitability of various NSAs for use as anodes in low temperature hydrogen fuel cells.

3.1. Stability of NSAs in the presence of hydrogen or CO

We begin by describing how NSAs for hydrogen-related reactions can be chosen; later, we comment briefly on how this analysis can be extended to reactions where CO is also present. To identify NSAs with well-defined properties, it is desirable that the composition in the near-surface region be stable in hydrogen-rich environments at appropriate temperatures and pressures. This stability can be estimated using a simple procedure that has been described previously [16]. In brief, the procedure consists of first determining the surface composition of the NSA in vacuum (this can be estimated by analyzing the energy needed to move a solute atom from the bulk to the surface of the host metal, E_{seg} [33]) and then determining the effect of hydrogen adsorption on this composition. The latter determination can be made by comparing the inherent tendency of the NSA to resist compositional changes (determined by E_{seg}) to the hydrogen-induced driving force for a change in composition (estimated by the difference in hydrogen binding energies on the corresponding clean metals). In general, this procedure suggests that hydrogen will not induce surface segregation for most solute/host transition metal pairs, at least at low temperatures and pressures.

This stability analysis can be extended to a hydrogen fuel cell environment by applying the same procedure to CO-induced compositional changes. The range of B.E.s of CO across the pure transition metals is larger than is the corresponding range for hydrogen (the range of B.E.'s between Au and Ru, e.g., is 0.75 eV for H and 1.87 eV for CO); compared to hydrogen, CO will, therefore, possess a larger thermodynamic driving force for adsorbate-induced segregation. However, we nonetheless find that several NSAs will be relatively stable in CO-rich environments (Fig. 1).

3.2. Hydrogen binding energies and H_2 dissociation barriers

Detailed results for hydrogen binding energies and H_2 dissociation energetics on a variety of pure metals and NSAs are given in previous publications [14,16], and only a summary of the results is given here. Briefly, a significant gap in hydrogen binding energies exists between the noble metals and the other transition metals considered. This gap is bridged by the NSAs, which generally exhibit weaker hydrogen binding than do the corresponding pure host metals. In fact, the strength of hydrogen adsorption is so reduced on some NSAs that they actually bind H more weakly than do the noble metals.

As regards the kinetics of H_2 activation on transition metals, a remarkable trend is seen in the transition state energies for dissociation on both the noble metals and on selected NSAs. Although hydrogen is as weakly bound to many of the Pt- and Pd-terminated NSAs as it is to the noble metals (Cu, Ag, and Au), the transition state energy for H_2 dissociation on these NSAs is significantly lower than is the corresponding energy on the noble metals (Fig. 2). These results suggest that certain of the NSAs effectively combine weak binding of atomic hydrogen with facile dissociation of H_2. This unusual combination of properties implies that the NSAs may serve as highly effective hydrogen transfer catalysts by both allowing

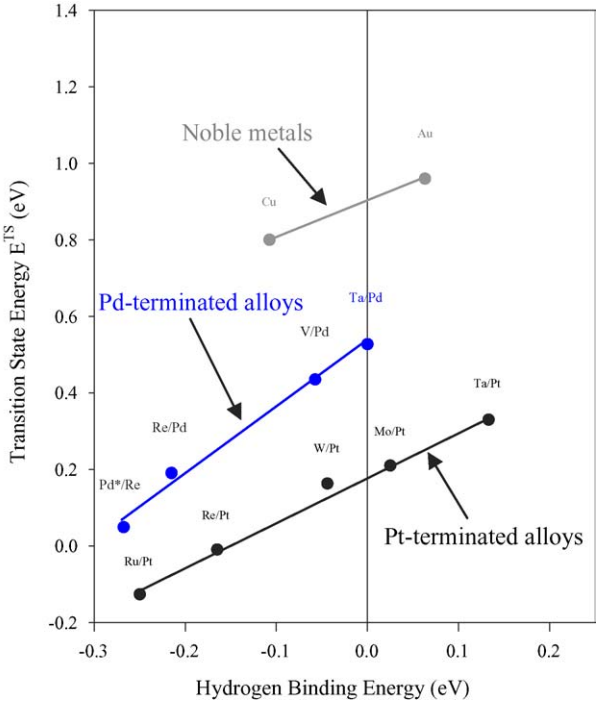

Fig. 2. Transition state (E^{TS}) energy vs. hydrogen binding energy for H_2 dissociation on (1 1 1) surfaces of pure noble metals and NSAs. The energy reference for both E^{TS} and the hydrogen B.E. corresponds to H_2(g) and the clean metal slab at infinite separation from one another.

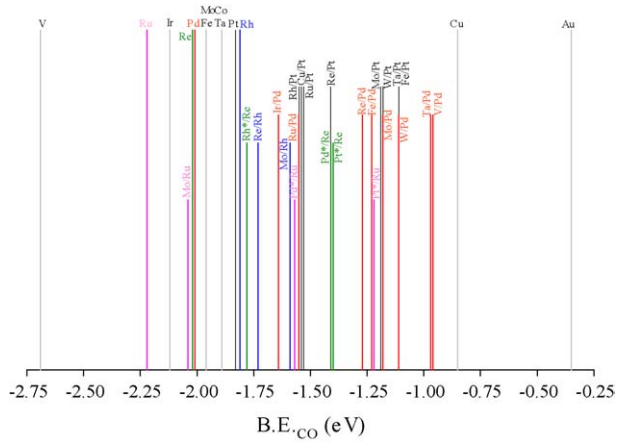

Fig. 3. CO binding energies (B.E.$_{CO}$) on various close-packed surfaces, referenced to a clean metal slab and a gas-phase CO molecule (CO(g)) at infinite separation from one another. Subsurface alloys are indicated with the notation solute/host, and overlayers are indicated as solute*/host. The height of the bars associated with the various alloys and pure metals is arbitrary and is varied only for clarity.

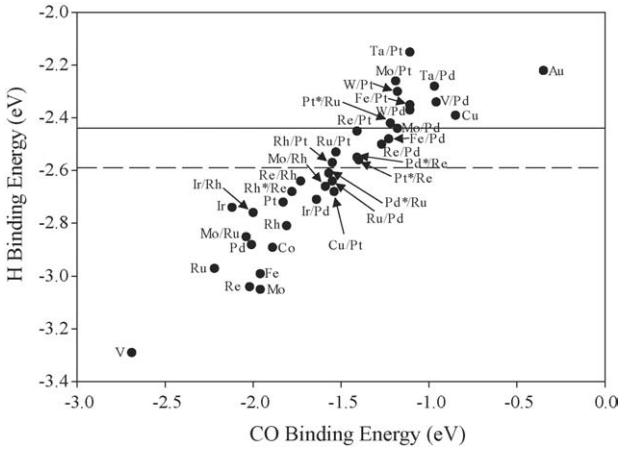

Fig. 4. Correlation between hydrogen and CO binding energies on close-packed surfaces of pure metals and NSAs. The hydrogen binding energy is referenced to a gas-phase hydrogen atom (H(g)), and the CO binding energy is referenced to a gas-phase CO molecule. The *solid* horizontal line denotes the hydrogen binding energy at which H_2 dissociation becomes spontaneous on Pt-terminated NSAs; the *dashed* horizontal line identifies the corresponding value for Pd-terminated NSAs.

ready dissociation of molecular hydrogen and making the resulting atomic hydrogen easily available for subsequent hydrogen transfer reactions.

3.3. CO binding energies

A schematic representation of the binding energies of CO on a variety of pure metals and on NSAs that are stable in CO-rich environments is given in Fig. 3, and the corresponding data are presented in Table A1 of the Appendix A. For the pure metals, a gap in binding energies between the noble metals and all other transition metals considered is clearly seen. This gap, which closely resembles the analogous gap seen for atomic hydrogen, is in large part filled by the CO binding energy on several NSAs. In addition, as was also the case with hydrogen, the binding of CO to the NSAs is generally weaker than is the CO binding to the corresponding host metals.

3.4. Combined H and CO binding energy analysis

The significant qualitative similarities between the hydrogen and CO binding characteristics on pure metals and NSAs suggest that a correlation might exist between the binding energies of these two adsorbates. Fig. 4 demonstrates that such a correlation does, in fact, exist; it is substantially linear. The correlation implies that there is a fundamental similarity between the electronic interactions of H and CO with metal surfaces. This similarity, in turn, can be traced back to the close relationship between the clean surface d-band centers and the binding energies of these two adsorbates [16,30].

4. Discussion

4.1. Fuel cell applications

The relationship between the hydrogen and carbon monoxide binding energies (Fig. 4) suggests an algorithm for screening NSAs for promising properties as fuel cell anodes. For the reasons described above, the anode must be resistant to CO poisoning. This property could be realized, for example, by finding alloys that bind CO weakly; NSAs with this property, and which are not suffering from CO-induced surface segregation, can easily be identified from Fig. 3. Weak binding of CO, however, implies that the anode will also bind hydrogen weakly (Fig. 4). This implication presents a potential problem for anode design because, for a hydrogen fuel cell anode to be useful, it must be able to activate H_2. According to Brønsted–Evans–Polanyi correlations for a number of simple dissociation reactions [17–19], weaker H binding should always imply a higher H_2 dissociation barrier. NSAs, however, permit an escape from that rule by offering, in some cases, the novel combination of weak hydrogen binding and facile H_2 activation [11,14,16]. This remarkable property suggests that they might be excellent candidates for hydrogen fuel cell anodes. Facile H_2 activation with weak hydrogen binding implies that H_2 activation could also be expected with weak CO binding (Fig. 3), thus presenting an almost ideal set of properties for these anodes.

To quantify the above speculations, we have used kinetic data from [16] (see also Fig. 2 of the present manuscript) to estimate the weakest hydrogen binding that would still be expected to result in quasi-spontaneous H_2 dissociation on Pt- and Pd-terminated NSAs. The resulting values, −2.44 eV for Pt-terminated NSAs and −2.59 eV for Pd-terminated NSAs, are indicated by horizontal lines in Fig. 4 (we note that inclusion of zero-point energy effects for adsorbed atomic hydrogen would simply shift both these lines and all of the data points along the hydrogen axis by the approximately constant amount of 0.15 eV; corresponding shifts along the CO axis, resulting from CO zero-point energies, would be smaller). Pt-terminated alloys located either at or immediately below the Pt-terminated horizontal line in that figure would be expected

to possess the lowest possible CO binding energy that still permits quasi-spontaneous H_2 activation. Pd-terminated alloys near the Pd-terminated horizontal line in Fig. 4 would, in turn, identify the best possible Pd-terminated NSAs. The results suggest that promising NSAs for hydrogen fuel cell anodes (both subsurface alloys and overlayers) are Ru/Pt, Pt*/Ru, Re/Pt, Pt*/Re, Rh/Pt, Pd*/Ru, Ru/Pd, Pd*/Re and possibly Cu/Pt.

We note that several bulk forms of the above binary alloys (most notably PtRu) are well known for their excellent performance as fuel cell anodes [31–34]. This fact suggests that our analysis, based on simple, ideal, NSAs is capable of identifying bimetallic combinations that do, in fact, have good catalytic properties for hydrogen fuel cell applications. This result may, at first, seem surprising, as our near-surface alloys do not closely resemble the bulk alloys that are often seen in working fuel cells. However, even bulk alloys often show significant concentration changes near the surface, and they can thus resemble purely surface alloys in the surface regions [35,36]. Thus, it is possible that the promising near-surface alloy properties observed in the present work contribute, in some way, to the activity of the bulk alloy catalysts. We note, in passing, that the ideal, bimetallic NSAs that show promising anodic properties do so through purely ligand and strain effects; since there is only one kind of atom present on the surface of these NSAs, the bifunctional mechanism cannot contribute to their activity [32,37].

4.2. Special catalytic sites and non-ideal NSAs

The NSA structures described above are clearly idealizations of real NSAs. In reality, it is fairly uncommon for NSAs to have a pure solute monolayer in either the first or second metal layers. Subsurface alloys, for example, have host-enriched first layers and solute-enriched second layers, but these layers are generally not completely pure [35]. Calculations have shown, however, that modest deviations from ideality of this nature do not *qualitatively* change the unusual catalytic properties of NSAs [16]. Further, we argue that minute amounts of solute (with coverages much less than one monolayer), even at the impurity level, in the near-surface regions may form a new kind of highly reactive defect site (Fig. 5); although not explicitly recognized so far, these NSA-defect sites could have unusual catalytic properties in their own right and might be responsible for special catalyst-promotional effects recorded in the literature [38–44]. For instance, and as summarized in Fig. 2, these NSA-defect sites could offer an attractive combination of fast kinetics for bond-breaking/making events (through the promotional effect of the second metal) and simultaneous resistance to poisoning by reactants/products of these reactions. It is interesting to contrast these properties of NSA-defects with the properties of more typical defect sites, e.g., under-coordinated surface defect sites (e.g., steps, kinks) that are sometimes quickly poisoned through strong binding of reactants, products, or other surface reaction intermediates, thus playing no significant role under steady-state reactions conditions. Contrary to this, poison-resistant NSA-defects would remain very active in promoting catalysis under steady-state reaction conditions.

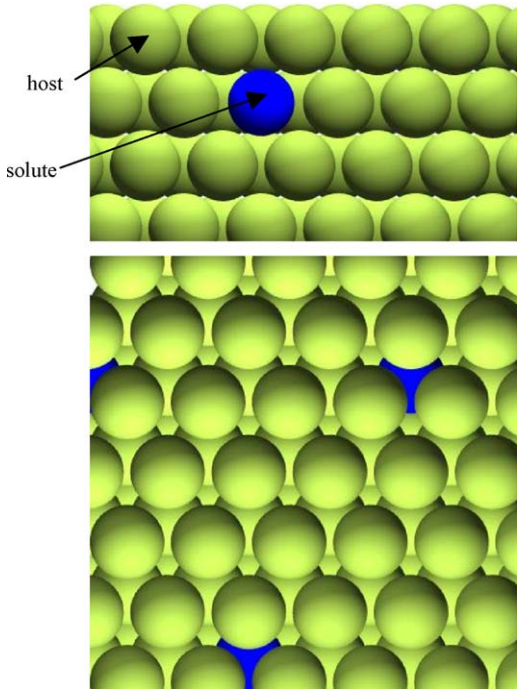

Fig. 5. Schematic representation of a NSA-defect site in cross-section and top-view. The light circles denote host metal atoms, while the dark circle indicates the subsurface solute impurity.

In any case, for both subsurface alloys with impure layers and isolated subsurface defects, deviations from ideality do produce *quantitative* changes in NSA properties. Thus, to fully benefit from the unique catalytic properties of NSAs, it will be necessary to achieve more precise control of metal catalyst surface structure, perhaps by implementing improved catalyst nanofabrication techniques. One such technique is Atomic Layer Deposition [45]; this approach can be applied to a variety of metal and oxide systems, including the deposition of well-defined metal films on porous oxide supports [46]. The success of this approach, together with techniques using dendrimers, electrochemical deposition of monolayers, and nanoparticle fabrication technologies, suggests that practical nanofabrication strategies for metals may not be far off [9,47–52].

5. Conclusions

Near-surface alloys possess a variety of unusual catalytic properties that could make them useful candidates for improved catalysts in a variety of chemical processes. It has already been shown in previous work that NSAs could facilitate highly selective hydrogen transfer reactions at low temperatures. In the present work, the list of potential applications for NSAs has been extended to low temperature hydrogen fuel cell anodes. The existence of a correlation between hydrogen and carbon monoxide binding energies on a variety of pure metals and NSAs has been established; this correlation, when coupled with kinetic data on H_2 dissociation from previous work, suggests that some NSAs, such as Ru/Pt, Pt*/Ru, Re/Pt, Pt*/Re, Rh/Pt,

Pd*/Ru, Ru/Pd, Pd*/Re and possibly Cu/Pt, have the combined properties of weak binding of CO with relatively facile H_2 activation. These properties, in turn, are ideal for anodes in hydrogen fuel cells. Accordingly, we suggest that, as nanoscale materials' synthesis techniques improve, it will become feasible to reproducibly prepare NSAs with highly specified surface structures, resulting in the design and manufacture of a wide variety of such materials for use in an ever increasing range of catalytic applications. Finally, we argue that at the dilute limit of NSAs, one can access the unique properties of a new kind of special NSA-defect sites, combining weak binding with facile bond-breaking/making. These special defect sites should be able to promote catalysis at a locally, poison-resistant environment, and under steady-state conditions.

Acknowledgements

This paper is dedicated to the 60th birthday of Henrik Topsøe and the 40th anniversary of Jens Rostrup-Nielsen with Haldor Topsøe S/A. DOE-BES has supported our work through a Hydrogen fuel Initiative grant to M.M. (DE-FG02-05ER15731). Calculations were performed with National Energy Research Scientific Computing Center (NERSC) and Molecular Science Computing Facility (MSCF-PNNL) resources. We thank Rahul Nabar for kind assistance with the graphics.

Appendix A

Table A1.

Table A1
Binding energies of CO on close-packed surfaces of pure metals, overlayers, and subsurface alloys

Metal or NSA	$B.E._{CO}$ (eV)	Metal or NSA	$B.E._{CO}$ (eV)
Au	−0.35	Ta/Pd	−0.97
Ir	−2.12	V/Pd	−0.96
Pt	−1.83	W/Pd	−1.11
Cu	−0.85	Re/Pd	−1.27
Re	−2.02	Mo/Pd	−1.18
Rh	−1.81	Fe/Pd	−1.23
Ru	−2.22	Ir/Pd	−1.64
Pd	−2.01	Ru/Pd	−1.55
Co	−1.89	Re/Rh	−1.73
Mo	−1.96	Ir/Rh	−2.00
Fe	−1.96	Mo/Rh	−1.59
V	−2.69	Mo/Ru	−2.04
W/Pt	−1.18	Pt*/Ru	−1.22
Ta/Pt	−1.11	Pd*/Ru	−1.57
Re/Pt	−1.41	Pt*/Re	−1.40
Mo/Pt	−1.19	Pd*/Re	−1.41
Fe/Pt	−1.11	Rh*/Re	−1.78
Ru/Pt	−1.53		
Rh/Pt	−1.55		
Cu/Pt	−1.54		

For all alloys, the first element listed is the solute, and the second element is the host. Asterisks (*) denote ideal overlayer NSAs; remaining NSAs are ideal subsurface alloys (see schematics in Fig. 1). The pure metals and each family of NSAs are listed in order of increasing d-band center (ε_d) of the corresponding clean surface.

References

[1] G.A. Somorjai, Introduction to Surface Chemistry and Catalysis, John Wiley, New York, 1994.
[2] I. Chorkendorff, J.W. Niemantsverdriet, Concepts of Modern Catalysis and Kinetics, WILEY-VCH, Weinheim, 2003.
[3] F. Besenbacher, I. Chorkendorff, B.S. Clausen, B. Hammer, A.M. Molenbroek, J.K. Nørskov, I. Stensgaard, Science 279 (1998) 1913.
[4] C.J.H. Jacobsen, S. Dahl, B.S. Clausen, S. Bahn, A. Logadottir, J.K. Nørskov, J. Am. Chem. Soc. 123 (2001) 8404.
[5] T. Zambelli, J. Wintterlin, J. Trost, G. Ertl, Science 273 (1996) 1688.
[6] J.H. Sinfelt, Bimetallic Catalysts: Discoveries, Concepts and Applications, John Wiley and Sons, New York, 1983.
[7] J.A. Rodriguez, D.W. Goodman, Science 257 (1992) 897.
[8] J.C. Vickerman, K. Christmann, G. Ertl, J. Catal. 71 (1981) 175.
[9] J. Zhang, M.B. Vukmirovic, Y. Xu, M. Mavrikakis, R.R. Adzic, Angew. Chem. Int. Ed. 44 (2005) 2132.
[10] M. Beutl, J. Lesnik, K.D. Rendulic, R. Hirschl, A. Eichler, G. Kresse, J. Hafner, Chem. Phys. Lett. 342 (2001) 473.
[11] H.H. Hwu, J. Eng Jr., J.G. Chen, J. Am. Chem. Soc. 124 (2002) 702.
[12] S. Hsieh, D. Beck, T. Matsumoto, B.E. Koel, Thin Solid Films 466 (2004) 123.
[13] J. Greeley, J.K. Nørskov, M. Mavrikakis, Ann. Rev. Phys. Chem. 53 (2002) 319.
[14] J. Greeley, M. Mavrikakis, J. Phys. Chem. B 109 (2005) 3460.
[15] J.R. Kitchin, J.K. Nørskov, M.A. Barteau, J.G. Chen, J. Chem. Phys. 120 (2004) 10240.
[16] J. Greeley, M. Mavrikakis, Nat. Mater. 3 (2004) 810.
[17] J.K. Nørskov, T. Bligaard, A. Logadottir, S. Bahn, L.B. Hansen, M. Bollinger, H. Bengaard, B. Hammer, Z. Sljivancanin, M. Mavrikakis, Y. Xu, S. Dahl, C.J.H. Jacobsen, J. Catal. 209 (2002) 275.
[18] Y. Xu, A.V. Ruban, M. Mavrikakis, J. Am. Chem. Soc. 126 (2004) 4717.
[19] A. Michaelides, Z.P. Liu, C.J. Zhang, A. Alavi, D.A. King, P. Hu, J. Am. Chem. Soc. 125 (2003) 3704.
[20] B. Hammer, J.K. Nørskov, Nature 376 (1995) 238.
[21] W. Vielstich, A. Lamm, H.A. Gasteiger (Eds.), Handbook of Fuel Cells: Fundamentals, Technology, Applications, Wiley, West Sussex, 2003.
[22] R.R. Davda, J.A. Dumesic, Angew. Chem. Int. Ed. 42 (2003) 4068.
[23] B. Hammer, L.B. Hansen, J.K. Nørskov, Phys. Rev. B 59 (1999) 7413.
[24] L. Bengtsson, Phys. Rev. B 59 (1999) 12301.
[25] D. Vanderbilt, Phys. Rev. B 41 (1990) 7892.
[26] J.P. Perdew, J.A. Chevary, S.H. Vosko, K.A. Jackson, M.R. Pederson, D.J. Singh, C. Fiolhais, Phys. Rev. B 46 (1992) 6671.
[27] J.A. White, D.M. Bird, Phys. Rev. B 50 (1994) 4954.
[28] G. Kresse, Furthmuller, J. Comput. Mater. Sci. 6 (1996) 15.
[29] CRC Handbook of Chemistry and Physics, 76th ed., CRC Press, New York, 1996.
[30] B. Hammer, Y. Morikawa, J.K. Nørskov, Phys. Rev. Lett. 76 (1996) 2141.
[31] K. Williams, T. Burstein, Catal. Today 38 (1997) 401.
[32] P. Liu, A. Logadottir, J.K. Nørskov, Electrochim. Acta 48 (2003) 3731.
[33] A. Hamnett, Catal. Today 38 (1997) 445.
[34] S.R. Brankovic, J.X. Wang, R.R. Adžic, Electrochem. Solid-State Lett. 4 (2001) A217.
[35] J.C. Bertolini, P. Delichère, P. Hermann, Surf. Interface Anal. 24 (1996) 34.
[36] J.R. Kitchin, N.A. Khan, M.A. Barteau, J.G. Chen, B. Yakshinksiy, T.E. Madey, Surf. Sci. 544 (2003) 295.
[37] P. Waszczuk, G.Q. Lu, A. Wieckowski, C. Lu, C. Rice, R.I. Masel, Electrochim. Acta 47 (2002) 3637.
[38] B. Klötzer, W. Unterberger, K. Hayek, Surf. Sci. 532–535 (2003) 142.
[39] R. Schennach, A. Eichler, K.D. Rendulic, J. Phys. Chem. B 107 (2003) 2552.
[40] C. Keresszegi, T. Mallat, J.D. Grunwaldt, A. Baiker, J. Catal. 225 (2004) 138.

[41] A. Sarkany, Z. Zsoldos, G. Stefler, J.W. Hightower, L. Guczi, J. Catal. 157 (1995) 179.
[42] T.B.L.W. Marinelli, S. Nabuurs, V. Ponec, J. Catal. 151 (1995) 431.
[43] P. Kappen, J.D. Grunwaldt, B.S. Hammershoi, L. Troger, B.S. Clausen, J. Catal. 198 (2001) 56.
[44] C. Keresszegi, J.D. Grunwaldt, T. Mallat, A. Baiker, J. Catal. 222 (2004) 268.
[45] B.S. Lim, A. Rahtu, R.G. Gordon, Nat. Mater. 2 (2003) 749.
[46] M.J. Pellin, P.C. Stair, G. Xiong, J.W. Elam, J. Birrell, L. Curtiss, S.M. George, C.Y. Han, L. Iton, H. Kung, M. Kung, H.H. Wang, Catal. Lett. 102 (2005) 127.
[47] R.W. Scott, A.K. Datye, R.M. Crooks, J. Am. Chem. Soc. 123 (2003) 3708.
[48] D.S. Deutsch, G. Lafaye, D. Liu, B.D. Chandler, C.T. Williams, M.D. Amiridis, Catal. Lett. 97 (2004) 139.
[49] S.R. Brankovic, J.X. Wang, R.R. Adzic, Surf. Sci. 474 (2001) L173.
[50] S.R. Brankovic, J. McBreen, R.R. Adzic, Electroanal. Chem. 503 (2001) 99.
[51] S. Zhou, B. Varughese, B. Eichhorn, G. Jackson, K. McIlwrath, Angew. Chem. Int. Ed. 44 (2005) 4539.
[52] Y. Vasquez, A.K. Sra, R.E. Schaak, J. Am. Chem. Soc. 127 (2005) 12504.